BIOCHEMISTRY
including biophysical chemistry & molecular biology

Article

pubs.acs.org/biochemistry

# Red/Green Cyanobacteriochromes: Sensors of Color and Power

Nathan C. Rockwell, Shelley S. Martin, and J. Clark Lagarias*

Department of Molecular and Cellular Biology, University of California, Davis, California 95616, United States

Supporting Information

**ABSTRACT:** Phytochromes are red/far-red photoreceptors using cysteine-linked linear tetrapyrrole (bilin) chromophores to regulate biological responses to light. Light absorption triggers photoisomerization of the bilin between the 15*Z* and 15*E* photostates. The related cyanobacteriochromes (CBCRs) extend the photosensory range of the phytochrome superfamily to shorter wavelengths of visible light. Several subfamilies of CBCRs have been described. Representatives of one such subfamily, including AnPixJ and NpR6012g4, exhibit red/green photocycles in which the 15*Z* photostate is red-absorbing like that of phytochrome but the 15*E* photoproduct is instead green-absorbing. Using recombinant expression of individual CBCR domains in *Escherichia coli*, we fully survey the red/green subfamily from the cyanobacterium *Nostoc punctiforme*. In addition to 14 new photoswitching CBCRs, one apparently photochemically inactive protein exhibiting intense red fluorescence was observed. We describe a novel orange/green photocycle in one of these CBCRs, NpF2164g7. Dark reversion varied in this panel of CBCRs; some examples were stable as the 15*E* photoproduct for days, while others reverted to the 15*Z* dark state in minutes or even seconds. In the case of NpF2164g7, dark reversion was so rapid that reverse photoconversion of the green-absorbing photoproduct was not significant in restoring the dark state, resulting in a broadband response to light. Our results demonstrate that red/green CBCRs can thus act as sensors for the color or intensity of the ambient light environment.

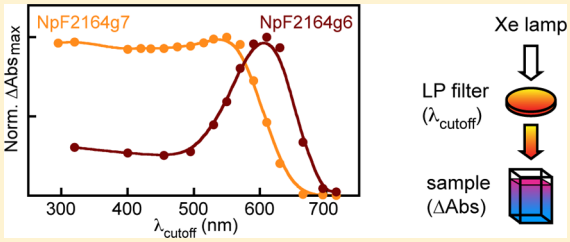


Nearly all organisms can respond to their light environment, inducing a broad range of photobiological responses such as adaptation to the diurnal cycle. Photosynthetic organisms are also able to adapt to different colors and intensities of light to optimize their metabolism for the ambient light environment.[4−9] Such photobiological responses are mediated by photosensory proteins, which typically use a range of organic molecules as accessory chromophores depending on the spectral response of the photoreceptor. Photosensors detecting near-UV to blue light[a] often use flavins or *p*-coumaric acid,[7] but vitamin B12 and pterins have also been recently implicated in such responses.[10,11]

Sensing longer wavelengths of light can instead use several linear tetrapyrroles [bilins (Figure S1 of the Supporting Information)] derived from the oxidative degradation of heme. Bilins are uniquely well suited to sensing light in the red and far-red regions of the spectrum, regions that match the absorption maxima of chlorophyll-based light-harvesting systems and photosynthetic reaction centers. The first bilin-based photoreceptors to be discovered were the phytochromes of higher plants,[12] which have a covalently attached bilin chromophore bound within a conserved pocket in a GAF domain.[13−15] This GAF domain is part of a knotted PAS-GAF-PHY photosensory core module[16−18] conserved in phytochromes from a wide range of organisms, including desmid algae, cyanobacteria, nonoxygenic photosynthetic bacteria, diatoms, nonphotosynthetic bacteria, and fungi.[19−26] Phytochromes use photoisomerization of the bilin 15,16-double bond to convert between red-absorbing (15*Z* $P_r$) and far-red-absorbing (15*E* $P_{fr}$) photostates, and the photosensory core module is sufficient for the native red/far-red[b] photocycle.[1,17,18,27−30] In most phytochromes, $P_{fr}$ is metastable and can decay thermally to $P_r$ in a process known as dark reversion.[27,31]

In addition to knotted phytochromes, cyanobacteria also contain knotless phytochromes containing a GAF-PHY photosensory core module.[14,32,33] Such knotless phytochromes retain red/far-red photocycles. Cyanobacteria also contain related sensors termed cyanobacteriochromes (CBCRs), which require only the GAF domain for autocatalytic attachment of a conserved Cys residue to the bilin chromophore and for photoconversion.[1,34,35] Several subfamilies of CBCRs have been described, all of which utilize phycocyanobilin [PCB (Figure S1A of the Supporting Information)] as the chromophore precursor.[1,35,36] In one CBCR subfamily, characterized by the presence of a loosely conserved DXCF motif containing a second Cys residue,[37] the covalent adduct formed from PCB can slowly isomerize to phycoviolobilin [PVB (Figure S1B of the Supporting Information)],[3,38] which absorbs at shorter wavelengths. Representatives of both DXCF and insert-Cys[36] subfamilies use second Cys residues to form covalent linkages to the C10 atom of the bilin chromophore (Figure S1B of the Supporting Information). This considerably shortens the conjugated system, allowing detection of blue, violet, or

**Received:** October 4, 2012
**Revised:** November 14, 2012
**Published:** November 14, 2012

Table 1. Spectral Parameters for Red/Green CBCRs from *N. punctiforme*[a]

| protein | bilin | native 15*Z* | 15*Z* CD | native 15*E* | denatured |
|---|---|---|---|---|---|
| NpAF142g2 | PCB | 356 (+), 650 (−) | weak | 532 (−) | 676, 574 |
| NpR4776g2 | PCB | 360 (+), 652 (−) | medium | 538 (−) | 671, 577 |
| NpR4776g2[b] | PΦB | 366, 666 | – | 550 | 678, – |
| NpR4776g3 | PCB | 356 (+), 656 (−) | medium | 558 (−) | 674, 578 |
| NpR6012g2[c] | PCB | 356, 650 | – | 556 | – |
| NpR6012g3 | PCB | 356 (+), 634 (−) | strong | 536 (−) | 678, 578 |
| NpR6012g4 | PCB | 356 (+), 652 (−) | medium | 538 (−) | 673, 574 |
| NpR6012g4 | PΦB | 368 (+), 666 (−) | medium | 552 (−) | 682, 592 |
| NpF2164g4 | PCB | 356 (+), 646 (−) | medium | 530 (−) | 676, 577 |
| NpF2164g5[d] | PCB | 350 (+), 640 (−) | strong | – | 662, – |
| NpF2164g6 | PCB | 354 (+), 648 (−) | weak | 546 (−) | 676, 580 |
| NpF2164g7[b] | PCB | 352 (+), 608 (−) | strong | 542 | 662, – |
| NpF2854g1 | PCB | 352 (+), 656 (−) | weak | 544 (−) | 676, 580 |
| NpF2854g2 | PCB | 354 (+), 656 (−) | weak | 542 (−) | 672, 588 |
| NpF2854g3 | PCB | 356 (+), 656 (−) | medium | 546 (−) | 672, 576 |
| NpR1597g4 | PCB | 350 (+), 640 (−) | strong | 550 (566, −) | 676, 582 |
| NpR1597g4 | PΦB | 358 (+), 650 (−) | strong | 550 (568, −) | 686, 598 |
| NpR5113g2 | PCB | 354 (+), 650 (−) | strong | 528 (−) | 672, 576 |
| NpR3784 | PCB | 352 (+), 652 (−) | strong | 554 (−) | 674, 576 |

[a]Peak wavelengths are reported in nanometers and were calculated from photochemical difference spectra, with the CD sign in parentheses for the native transitions. CD peak wavelengths are reported in parentheses for transitions in which the peak wavelength observed by CD is ≥10 nm different from that observed by difference spectroscopy. The 10 nm cutoff was derived by analyzing peak wavelengths for recently published CBCRs.[3,36,40,46] In this set, the mean offset between absorbance and CD peak wavelengths was 0.6 ± 8.4 nm (standard deviation; $n = 30$). The 15*E* Soret transition is not resolved in difference spectra, and its CD band overlaps that of the band at approximately 280 nm; as a result, peak wavelengths are not reported. However, in all cases, this transition exhibits positive CD. Denatured peak wavelengths are reported for the long-wavelength transition as 15*Z*, 15*E* pairs. The CD intensity for the 15*Z* photostate was classified as strong, weak, or medium by dividing the peak CD for the long-wavelength band by that of the Soret band and taking the absolute value of the resulting ratio. Values of <0.4, 0.4−0.6, and >0.6 meant the CD was considered weak, medium, and strong, respectively. [b]Photoproduct CD and denatured spectra could not be resolved because of rapid dark reversion. The denatured value is for the absorbance spectrum. [c]CD spectroscopy and denaturation analysis were not feasible because of poor protein stability. [d]Photoconversion was not detected, so peak wavelengths are reported for absorbance spectra rather than difference spectra.

ultraviolet light by the red-absorbing PCB or green-absorbing PVB. CBCRs thus have much more diverse ground-state chemistries and spectral responses than phytochromes, exhibiting an astonishing variety of photocycles reported to date. Despite this diversity, all CBCRs thus far reported retain photoisomerization at the bilin C15 methine bridge (Figure S1A of the Supporting Information) as the primary photochemical mechanism for photoperception.[3,35,36,39,40]

Other CBCR subfamilies do not have second Cys residues and typically retain the ability to respond to red light. In the case of cyanobacterial complementary chromatic adaptation sensors,[4,41] the 15*Z* photostate responds to green light ($^{15Z}P_g$) and is converted to the red-absorbing $^{15E}P_r$ photostate in a green/red photocycle.[42,43] In AnPixJ, slr1393, and NpR6012g4, the 15*Z* photostate instead absorbs red light ($^{15Z}P_r$) and is converted to $^{15E}P_g$ in a reversed red/green photocycle.[44−46] Such red/green CBCRs exhibit conserved sequence motifs that are distinct from those of phytochromes, green/red CBCRs, and DXCF CBCRs (Figure S2 of the Supporting Information). The insert-Cys CBCRs are apparently closely related to red/green CBCRs but contain a large insert containing their second Cys residue.[36] However, at least one member of the red/green subfamily defined by protein sequence has been reported to exhibit an anomalous photocycle with a red-shifted photoproduct with very fast dark reversion.[31] This result demonstrates that greater photochemical diversity exists within the red/green CBCR subfamily.

Our understanding of the relationship between the CBCR primary sequence and observed photocycle will be improved by greatly expanding the number of characterized sequences. In this regard, we have characterized all members of the red/green CBCR subfamily from the filamentous cyanobacterium *Nostoc punctiforme* ATCC 29133, consisting of 15 proteins. Most of these proteins vary only slightly in peak wavelength, yet variations in chromophore incorporation and photochemical efficiency were observed. Both $^{15Z}P_r$ and $^{15E}P_g$ photostates exhibit heterogeneity, and the rate of dark reversion varies greatly among subfamily members. Dark reversion in one of these CBCRs is so rapid that color preference is lost, resulting in a protein with the properties of a broadband power sensor.

## MATERIALS AND METHODS

**Bioinformatics.** BLAST searches used AnPixJ and NpR6012g4 as query sequences to identify putative red/green CBCRs encoded within the genome of *N. punctiforme*.[44,46,47] Multiple-sequence alignments were performed using MUSCLE[48] for an initial alignment. We subsequently combined that alignment with alignments of other subfamilies.[3,36] Final manual adjustment of the resulting alignment used conserved residues, highlighted in Figure S2 of the Supporting Information.

**Cloning and Expression of CBCRs.** Specific protein regions cloned for expression are reported in Figure S3A of the Supporting Information. Appropriate primers were used to amplify regions of interest from *N. punctiforme* genomic DNA, and polymerase chain reaction products were digested with *Nco*I and *Sma*I to permit cloning into pBAD-Cph1-CBD.[49] The resulting C-terminal intein−CBD fusion proteins were coexpressed with pPL-PCB, encoding biosynthetic machinery for PCB production, in *E. coli* strain LMG194.[50] Coproduction of


dx.doi.org/10.1021/bi3013565 | *Biochemistry* 2012, 51, 9667−9677

PΦB used a published modification of this system.[51] Purification using chitin resin (NEB) followed the manufacturer's directions with previously published modifications, with final dialysis against TKKG buffer [25 mM TES-KOH (pH 7.8), 100 mM KCl, and 10% (v/v) glycerol].[49] Spectroscopic parameters for purified proteins are listed in Table 1 and Table S1 of the Supporting Information.

Purified protein was analyzed by sodium dodecyl sulfate−polyacrylamide gel electrophoresis using standard procedures and apparatus (Bio-Rad) followed by semidry transfer to PVDF membranes, staining with amido black for visualizing total protein, and zinc blotting[52] to confirm the presence of covalently bound bilin (Figure S3B of the Supporting Information). Some proteins were concentrated using centrifugal concentrators (10 kDa cutoff, Amicon) prior to analysis. All constructs were verified by nucleotide sequencing.

**Spectroscopic Characterization of CBCRs.** Absorbance spectra were recorded at 25 °C on a Cary 50 spectrophotometer modified for illumination from above with a 75 W xenon source passed through a water filter and then through bandpass or long-pass filters.[49] Bandpass filters used for triggering photochemistry had center and width ((fwhm)) values of 670 and 40 nm, 650 and 40 nm, 600 and 40 nm, 550 and 70 nm, and 500 and 25 nm, respectively. Long-pass filters (Schott) were purchased from Edmund Industrial Optics. RG715, RG695, RG665, RG630, RG610, OG590, OG570, OG550, OG530, OG515, GG495, GG475, GG455, GG435, GG420, GG400, WG320, and WG295 filters were used. CD spectra were acquired on an Applied Photophysics Chirascan as described previously.[36] Denaturation assays used a 1:6 dilution with 6 M guanidinium chloride and 100 mM citric acid (pH 2.2).[53] All photochemical difference spectra are reported as 15*Z* − 15*E*. Extinction coefficients were derived from the absorbance spectra in two steps. The holoprotein concentration was estimated using the extinction coefficient for PCB ($\varepsilon_{662}$ = 35500) under acidic denaturing conditions.[54,55] The native absorbance spectra were then corrected for holoprotein concentration using the Beer−Lambert law to give the native extinction coefficients reported in Table S1 of the Supporting Information.

**Measurement of Dark Reversion.** For NpR4776g2, NpR4776g3, NpF2164g6, NpF2164g7, and NpR1597g4, dark reversion was measured at 25 °C by incubating the 15*E* photostate in darkness with acquisition of absorbance at single wavelengths (NpF2164g7 and the PΦB adduct of NpR4776g2) or of absorption spectra (all other proteins). Dark reversion of other proteins was too slow for this procedure to be practical. For these proteins, the 15*E* photostate was incubated in darkness at room temperature, and absorption spectra were taken on aliquots at 25 °C. For all proteins, data at selected wavelengths were fit to single-exponential models with floating end points by nonlinear regression.

## RESULTS

**Characterization of the Red/Green CBCR Subfamily from *N. punctiforme*.** Known examples of red/green CBCRs[31,44−46] contain several characteristic amino acid substitutions that distinguish them from phytochromes and from DXCF CBCRs, including a DX(Y/H)LQ motif aligned with the DIP motif of phytochromes and with the signature motif of DXCF CBCRs (Figure S2 of the Supporting Information). We used BLAST searches with AnPixJ and NpR6012g4, previously characterized red/green CBCRs,[44,46] to identify additional candidates within the *N. punctiforme* genome. Fourteen such domains were identified in seven open reading frames (Figure 1), including NpR6012g4 itself.

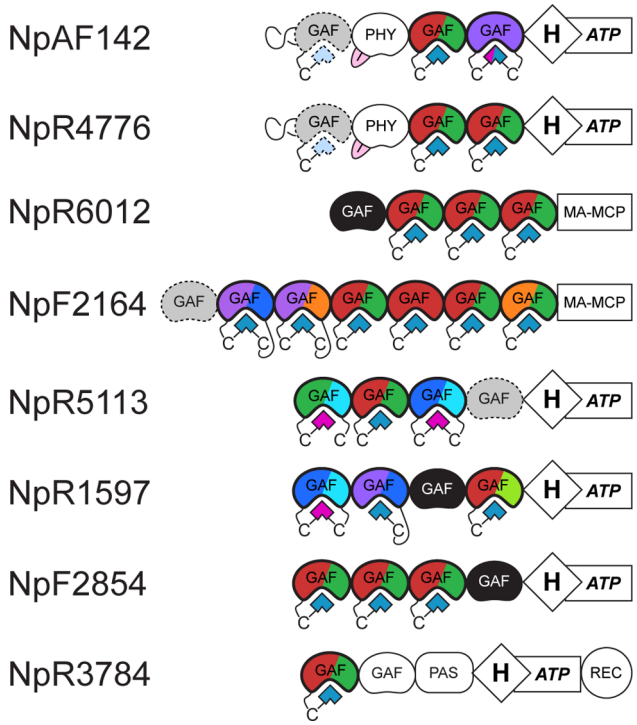


**Figure 1.** Domain structures of red/green CBCRs from *N. punctiforme*. CBCRs are color-coded by photocycle, including members of the insert-Cys, DXCF, and red/green subfamilies.[3,36,46] The polygon below the GAF domain represents the bilin (blue for PCB and pink for PVB). GAF domains that fail to bind bilin but that are related to DXCF CBCRs are colored black, and undescribed GAF domains are colored gray with a black dashed outline. REC domains, MA-MCP domains, and His kinase domains (indicated by H-ATP) are involved in two-component signaling pathways.

We also found a single CBCR with sequence characteristics of both red/green and DXCF CBCRs, NpR3784 (Figure 1 and Figure S2 of the Supporting Information). NpR3784 lacks the DXCF Cys residue required to make a second linkage to the chromophore in this subfamily.[3,37−40] As a first step in understanding the roles of these proteins in the photobiology of *N. punctiforme*, we expressed the individual CBCR domains recombinantly in *E. coli* engineered to produce PCB as chromophore precursor. We have used this approach to characterize the DXCF and insert-Cys CBCRs from *N. punctiforme*, along with the red/green CBCR NpR6012g4 from the same organism.[3,36,46] Recombinant CBCRs from cyanobacterial expression systems are similar to those expressed in *E. coli*, and truncated CBCRs have photocycles similar to those of the parent full-length proteins or larger soluble fragments.[3,34,35,37,42,43,56,57] We therefore expect this survey to provide useful insights into the properties of the individual CBCR domains, providing a knowledge base for understanding or designing more complex sensors or for shifting the spectral responses of existing pathways.

All 14 candidate CBCRs were expressed and purified individually. Despite good initial yield and robust photoconversion (Figure S3C of the Supporting Information), NpR6012g2[c] was the only CBCR that proved to be unstable


dx.doi.org/10.1021/bi3013565 | *Biochemistry* 2012, 51, 9667−9677

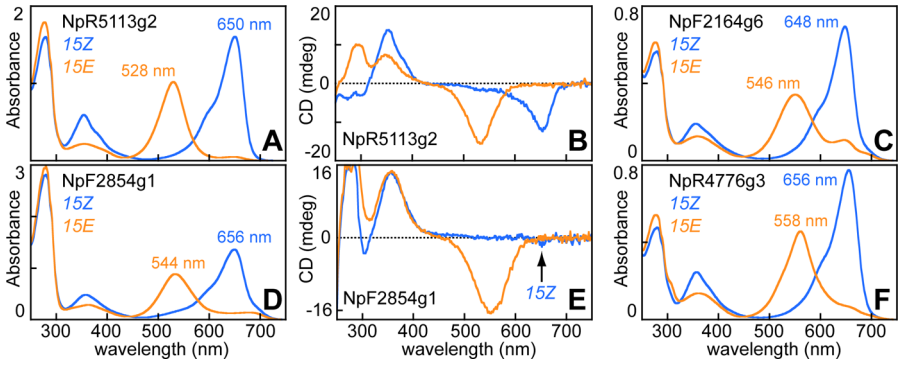


**Figure 2.** Characterization of red/green CBCRs from *N. punctiforme*. Absorption spectra are shown for NpR5113g2 (A), NpF2164g6 (C), NpF2854g1 (D), and NpR4776g3 (F) in the 15*Z* (blue) and 15*E* (orange) photostates. Peak wavelengths calculated from photochemical difference spectra are indicated and are reported in Table 1, and additional proteins are presented in Figure S4 of the Supporting Information. CD spectra are shown for NpR5113g2 (B) and NpF2854g1 (E) in the same color scheme to illustrate the variable signal intensity of the $^{15Z}P_r$ state. This state gives rise to a robust CD signal in NpR5113g2 but a weak signal in NpF2854g1 (arrow).

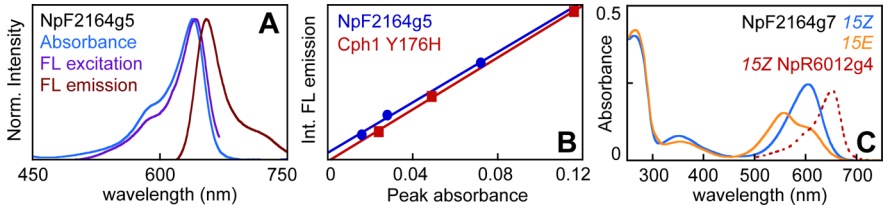


**Figure 3.** Red/green CBCRs with atypical $^{15Z}P_r$ photostates. (A) Normalized absorbance (blue), fluorescence excitation (purple), and fluorescence emission (red) spectra are shown for NpF2164g5. (B) Plot of integrated fluorescence emission vs peak absorbance for dilution series of NpF2164g5 (blue) and $Y_{176}H$ mutant Cph1 (red), which has a known fluorescence quantum yield.[51] The slopes of these lines are proportional to the quantum yields for fluorescence,[37] so the similar slopes of $Y_{176}H$ Cph1 NpF2164g5 indicate comparable quantum yields of 0.1−0.15. (C) Absorbance spectra of NpF2164g7 in the 15*Z* (blue) and 15*E* (orange) photostates. The 15*Z* state is blue-shifted relative to the $^{15Z}P_r$ states of proteins such as NpR6012g4 (dashed red). Peak wavelengths from the photochemical difference spectrum are listed in Table 1.

as assayed by rapid accumulation of scatter in absorbance spectra. We therefore did not further characterize this red/green CBCR, choosing to compare the other 13 with the previously characterized NpR6012g4.[46,58,59] Most of these new sensors exhibited red/green photocycles similar to those previously described (Figure 2 and Figure S4 of the Supporting Information), with peak wavelengths listed in Table 1 and other spectral parameters listed in Table S1 of the Supporting Information. For all CBCRs examined, denaturation analyses confirmed the presence of PCB and were consistent with photoisomerization of the C15,16 double bond (Table 1). As in previously published examples,[44−46] conversion from the red-absorbing dark state ($^{15Z}P_r$) to the green-absorbing photoproduct ($^{15E}P_g$) was accompanied by a change in intensity but no significant change in peak wavelength for the second (Soret) transition. Therefore, no separate wavelength is reported for the 15*E* Soret transition in Table 1. The red-absorbing dark state ($^{15Z}P_r$) typically exhibited only subtle differences in peak wavelength [634−656 nm (Table 1)], with all examples blue-shifted relative to the knotted cyanobacterial phytochrome Cph1.[20,49,51]

NpAF142g2, NpF2854g1, NpR4776g2, and NpR3784 all exhibited much lower levels of chromophore incorporation than other proteins (Figure 2 and Figure S4 and Table S1 of the Supporting Information). Such a result could indicate that these proteins are less suited to recombinant expression. NpAF142g2 exhibited noted heterogeneity in its dark reversion (Figure S5A of the Supporting Information). A minor population (approximately 10%) underwent dark reversion rapidly, with a red-shifted difference spectrum relative to the main population. The slower reverting majority population better matched the photochemical difference spectrum. While the former population was too small to allow identification by denaturation analysis, its absorption at longer wavelength is consistent with a noncovalently bound, photoactive bilin population. It is known that the bacterial phytochrome Agp1 can photoconvert noncovalently bound bilins.[60] Such a noncovalent population in NpAF142g2 would provide an explanation for the poor bilin incorporation of such proteins: they could exhibit intrinsically inefficient covalent attachment.

The intensity of CD signals from the red band of $^{15Z}P_r$ was quite variable (Figure 2 and Table 1). This result may reflect slight variations in D-ring geometry and/or protein−chromophore interactions in the different sensors. It could also arise from a heterogeneous mixture of $^{15Z}P_r$ species with similar absorption spectra but different CD intensities, consistent with the observed heterogeneity of the NpR6012g4 forward reaction on an ultrafast time scale.[46,58] To test this hypothesis, we examined forward photoconversion of NpR6012g4 and NpR5113g2 using brief pulses of red light (30 s to 1 min). Difference spectra for the initial part of the reaction and those obtained at the end were normalized on the $^{15E}P_g$ photoproduct band to allow facile comparison of the 15*Z* states (Figure S5B,C of the Supporting Information). In both proteins, this comparison revealed that more $^{15Z}P_r$ was required at the end of the reaction to generate the same amount of photoproduct. However, this assay did not reveal such an effect in NpR4776g3 (Figure S5D of the Supporting Information). The subtle change in photoconversion efficiency observed with NpR6012g4 and NpR5113g2 demonstrates that multiple red/


dx.doi.org/10.1021/bi3013565 | *Biochemistry* 2012, 51, 9667−9677

green CBCRs contain subpopulations with very similar peak wavelengths and line shapes but with differences in extinction coefficient, photochemical quantum yield, or both.

**CBCRs That Deviate from the Red/Green Photocycle.** We found two examples with atypical 15*Z* photostates: NpF2164g5 and NpF2164g7. First, NpF2164g5 exhibited an apparently normal $^{15Z}P_r$ photostate (Figure 3A), but photoconversion could not be detected (Figure S6A of the Supporting Information). Similar behavior has also been reported for two CBCR domains in *all1069*, also encoding AnPixJ.[44] Such behavior could arise via an extremely low quantum yield for forward photoconversion or via rapid dark reversion of an extremely unstable photoproduct. In this study, we were readily able to detect photoconversion in examples with dark reversion occurring as fast as 0.2 $s^{-1}$ (see below), implying much more rapid dark reversion in NpF2164g5 were photoconversion to occur at all. However, NpF2164g5 exhibited intense red fluorescence (Figure 3), with a quantum yield close to that of the well-characterized fluorescent $Y_{176}H$ mutant Cph1.[51,61] Second, NpF2164g7 exhibited a blue-shifted 15*Z* form at 608 nm, falling in the orange region of the visible spectrum (Figure 3C). Illumination of the 15*Z* NpF2164g7 ground state with orange light (600 ± 20 nm) resulted in incomplete formation of an apparently normal $^{15E}P_g$ photoproduct. Denaturation confirmed the presence of a PCB adduct, with no apparent PVB formation, and confirmed the incomplete nature of photoconversion (Figure S6 of the Supporting Information). In this case, incomplete conversion arose because of rapid dark reversion to the $^{15Z}P_o$ dark state (Table 2 and see below).

**Table 2. Dark Reversion Rates for Red/Green CBCRs from *N. punctiforme***

| protein | bilin | $t_{1/2}$ | $k_{DR}$ ($s^{-1}$) | error (%) |
|---|---|---|---|---|
| NpAF142g2 | PCB | 11 h | $1.7 \times 10^{-5}$ | 25 |
| NpR4776g2 | PCB | 25 s | 0.028 | 7 |
| NpR4776g2 | PΦB | 3.9 s | 0.18 | 6 |
| NpR4776g3 | PCB | 7.7 min | $1.5 \times 10^{-3}$ | 13 |
| NpR6012g4 | PCB | 33 h | $5.8 \times 10^{-6}$ | 33 |
| NpR6012g4 | PΦB | 6.4 h | $3.0 \times 10^{-5}$ | 25 |
| NpF2164g4 | PCB | 44 h | $4.4 \times 10^{-6}$ | 11 |
| NpF2164g6 | PCB | 1.2 min | 0.01 | 20 |
| NpF2164g7 | PCB | 4.1 s | 0.17 | 1.2 |
| NpF2854g1 | PCB | 15 h | $1.3 \times 10^{-5}$ | 43 |
| NpF2854g3 | PCB | 15 h | $1.3 \times 10^{-5}$ | 28 |
| NpR1597g4 | PCB | 3.9 h | $5.0 \times 10^{-5}$ | 12 |
| NpR1597g4 | PΦB | 1.5 h | $1.3 \times 10^{-4}$ | 40 |
| NpR5113g2 | PCB | 3.9 h | $5.0 \times 10^{-5}$ | 27 |
| NpR3784 | PCB | 1.4 h | $1.4 \times 10^{-4}$ | 26 |

In most red/green CBCRs in this study, the $^{15E}P_g$ photostate exhibited only slight differences in peak wavelength (Table 1). Two examples with longer peak wavelengths, NpR4776g3 and NpR3784, also exhibited a less symmetric $^{15E}P_g$ peak than did proteins such as NpR6012g4 or NpF2164g6 (Figure 2 and Figure S4 of the Supporting Information). Such differences in line shape could again reflect the underlying heterogeneity of the $^{15E}P_g$ photostate, which was observed in the NpR6012g4 reverse reaction using interleaved pump−probe spectroscopy.[59] We also found two examples with possibly anomalous photoproducts: NpR4776g2 and NpR1597g4.

NpR4776g2 exhibited poor chromophore incorporation and also possessed a photochemically inert long-wavelength-absorbing population (Figure 4A), possibly indicating the

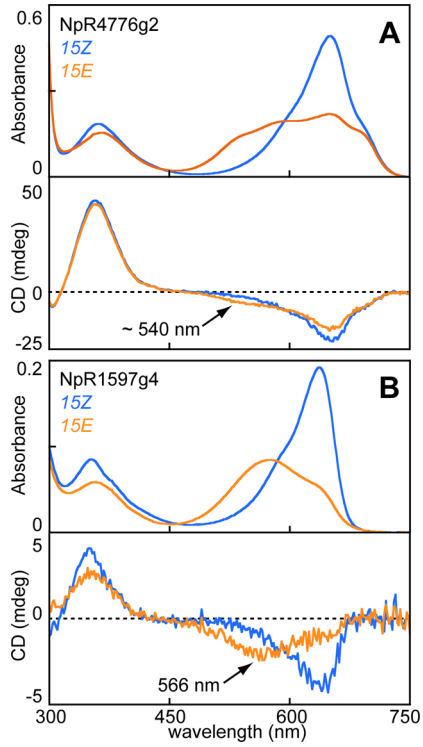


**Figure 4.** Red/green CBCRs with atypical $^{15E}P_g$ photostates. Absorbance (top) and CD (bottom) spectra are presented for NpR4776g2 (A) and NpR1597g4 (B) in the 15*Z* (blue) and 15*E* (orange) photostates. NpR4776g2 exhibited multiple possible photoproduct peaks via absorption spectroscopy, but the CD spectrum exhibited only one product at approximately 540 nm. By contrast, CD spectroscopy confirmed a red-shifted photoproduct in NpR1597g4.

presence of noncovalent bilin (see above). NpR4776g2 was poorly photoactive, yielding an apparent green-absorbing photoproduct and a possible second photoproduct absorbing in the vicinity of the isosbestic point (Figure 4A). However, both difference spectroscopy (Table 1) and CD spectroscopy (Figure 4A, bottom panel) provided support for a single photoproduct at approximately 540 nm. Incorporation of PΦB as a chromophore precursor resulted in red shifts nearly identical to those seen in NpR6012g4 (Figure S7 of the Supporting Information and Table 1), further supporting the idea that this protein has low photochemical efficiency but normal $^{15Z}P_r$ and $^{15E}P_g$ photostates.

NpR1597g4 exhibited an anomalous red-shifted photoproduct and potentially incomplete photoconversion (Figure 4B). The latter was confirmed by denaturation (Figure S6D of the Supporting Information). The $^{15E}P_g$ peak wavelength measured by difference spectroscopy was apparently normal (Table 1), but the red-shifted 15*E* photoproduct overlapped with the 15*Z* dark state. This overlap potentially confounds the use of difference spectroscopy for NpR1597g4. CD spectroscopy confirmed the presence of a red-shifted photoproduct peak at approximately 566 nm (Figure 4B, bottom panel). NpR1597g4 therefore possesses a photoproduct absorbing in the yellow region of the spectrum. A red-shifted photoproduct has also been reported for the CBCR domain of All2699,[31]


dx.doi.org/10.1021/bi3013565 | *Biochemistry* 2012, 51, 9667−9677

although in this case, a combination of rapid dark reversion and spectral overlap confounded analysis of the photoproduct band. Incorporation of PΦB as a chromophore precursor in NpR1597g4 did not result in a large red shift of the 15*E* photoproduct as measured by CD spectroscopy (Table 1), but we confirmed the presence of PΦB by denaturation and by a clear red shift of the 15*E* Soret band (Figure S7 of the Supporting Information). These data indicate that the red/green CBCR subfamily of *N. punctiforme* exhibits unexpected diversity, with a novel orange/green cycle found in NpF2164g7. However, there is less diversity in red/green CBCRs than in the members of the DXCF subfamily from the same organism,[3] with most proteins predicted to be red/green CBCRs by sequence alignment exhibiting the expected red/green photocycle.

**Red/Green CBCRs Function as Color or Intensity Sensors via Variation in Dark Reversion.** Previous reports of dark reversion in red/green CBCRs have implicated a broad range of rates.[31,59] We therefore examined dark reversion for the proteins in this study, except for NpF2164g5 (photochemically inactive), NpR6012g2 (unstable), and two other CBCRs, NpR6012g3 and NpF2854g2, that also proved to be unstable during long incubations. First-order rate constants for the other 12 proteins as PCB adducts were determined (Table 2). We observed great variation in dark reversion, which ranged from seconds to days depending on the protein (Figure 5).

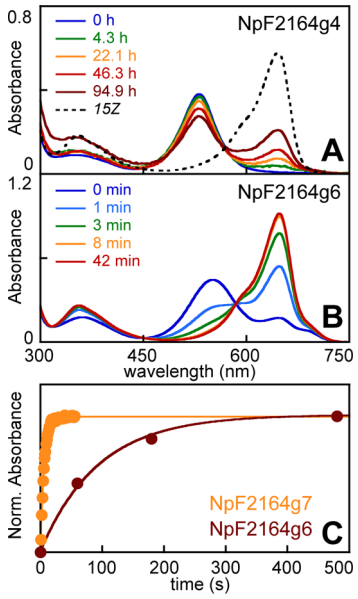


**Figure 5.** Dark reversion of red/green CBCRs. (A) NpF2164g4 was photoconverted from the $^{15Z}P_r$ state (– – –) to the $^{15E}P_g$ state (0 h, blue). Protein was then incubated at room temperature (~21 °C) in darkness for several days. At the indicated times, aliquots were removed and absorption spectra were acquired. (B) NpF2164g6 was photoconverted to the $^{15E}P_g$ state (time 0 min, blue). It was then incubated at 25 °C for several minutes, and absorption spectra were acquired at the indicated times. (C) Absorbance at the peak wavelength for the 15*Z* photostate plotted for NpF2164g6 (dark red) from the data shown in panel B. Equivalent data are also shown for a similar experiment performed with NpF2164g7 (orange), except that dark reversion was too rapid to permit acquisition of complete spectra. Instead, the absorbance was monitored at 600 nm. Both progress curves were described well by a single-exponential model, with rate constants and half-times listed in Table 2.

Substitution of PΦB for PCB (Figure S1A of the Supporting Information) produced a modest but significant increase in the dark reversion rate in all three tested examples (Figure S7D–F of the Supporting Information), which span a broad range of dark reversion rates (Table 2). This consistent effect of PΦB may indicate that the C18 side chain is normally twisted out of the D-ring plane in the $^{15E}P_g$ photostate, as would be expected for an ethyl moiety. Introduction of the vinyl moiety of PΦB would favor planarity of the C18 side chain to permit conjugation with the D-ring, possibly shifting the D-ring conformation and destabilizing the 15*E* photostate. NpR1597g4 exhibits a red-shifted 15*E* PCB photoproduct that is not further red-shifted by incorporation of PΦB (Table 1). The structural distortions that result in the red-shifted PCB photoproduct may therefore be absent or offset in the PΦB photoproduct. Offsetting movements of the D-ring and C18 side chain would reduce the red shift associated with PΦB at the cost of destabilizing the 15*E* photostate by forcing a high-energy conformation with the 18-vinyl out of conjugation. Such destabilization could again result in faster dark reversion, as in cases with normal $^{15E}P_g$ photoproducts.

With a dark reversion half-life of 4 s (Table 2), it is questionable whether NpF2164g7 would function as a color sensor. Such rapid dark reversion would reduce the importance of reverse photoconversion in determining the photostate. However, we reasoned that sufficiently rapid dark reversion could allow proteins to function as sensors of light intensity rather than of light quality (color). We therefore examined photoconversion as a function of power for NpF2164g6 and NpF2164g7 under red (650 ± 20 nm) and orange (600 ± 20 nm) light, respectively. Both proteins exhibited sufficiently rapid dark reversion to preclude complete photoconversion. Formation of $^{15E}P_g$ also was linear with power for both proteins, consistent with a function as intensity sensors (Figure S8A–C of the Supporting Information). Nevertheless, the use of specific wavelengths of light in this experiment does not demonstrate a loss of color specificity.

We therefore designed a new experiment to test whether the linear response to intensity was accompanied by a loss of color response in these two proteins (Figure 6). Light from a xenon lamp was used to trigger photoconversion with a series of long-pass filters with different cutoff lengths. A 715 nm cutoff yielded effectively no photoconversion for either protein. As the cutoff wavelength was shortened, forward photoconversion was observed as the incident light became resonant with the 15*Z* dark states (Figure 6). For NpF2164g6, a continued increase in the bandwidth resulted in a substantial reduction in the level of photoconversion, with <50% of maximal conversion observed with a 455 nm cutoff. This indicated that reverse photoconversion, and hence photochromism, remained significant factors in determining the photoequilibrium attained by NpF2164g6. By contrast, increasing the illumination bandwidth to the same point resulted in little loss of photoconversion for NpF2164g7 (Figure 6). Indeed, white light (320 or 285 nm cutoff wavelength) resulted in >95% of the maximal photoconversion observed with specific orange light. A cutoff of 610 nm was sufficient to allow approximately 50% of maximal photoconversion, indicating a broadband light response in NpF2164g7. We therefore conclude that dark reversion of NpF2164g7 [$k_{DR}$ = 0.17 $s^{-1}$ (Table 2)] is sufficiently rapid as to render reverse photoconversion insignificant in attaining photoequilibrium. This protein thus is no longer a sensor for color (orange and green photostates) but rather functions as a


dx.doi.org/10.1021/bi3013565 | *Biochemistry* 2012, 51, 9667–9677

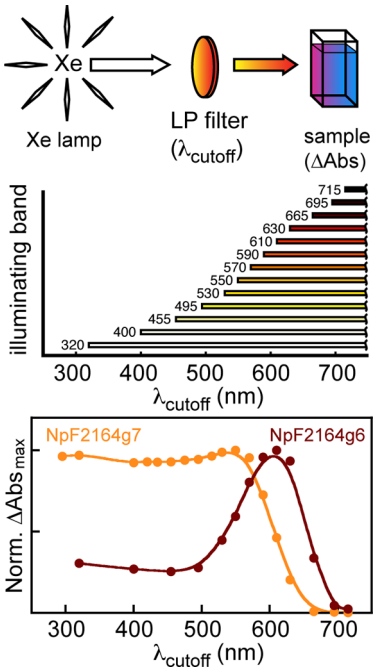


**Figure 6.** NpF2164g7 is a broadband photosensor. To assess photoconversion under broadband illumination (top), we used a series of long-pass filters with different cutoff wavelengths to filter the output of a xenon source, triggering photoconversion of NpF2164g6 and NpF2164g7 with the resulting light. Representative illumination bands generated by the apparatus in the top panel are shown in the middle panel. Photoconversion was measured as the maximal value of the photochemical difference spectrum obtained with each long-pass filter normalized to the maximum value obtained for each protein (bottom). Data thus vary from zero to one and can be compared for the two proteins. The level of photoconversion of NpF2164g6 (dark red) is reduced by addition of green light to the illuminating band, while that of NpF2164g7 (orange) is not.

broadband sensor of light intensity for incident wavelengths of ≤610 nm. These data thus demonstrate that CBCRs of the red/green subfamily can act as either color sensors or power sensors.

## DISCUSSION

In this work, we have characterized 14 new members of the red/green CBCR subfamily found in the genome of *N. punctiforme*, completing the description of this subfamily in this cyanobacterium. We have found 11 additional robust red/green photocycles; taken together with the previously described NpR6012g4,[46] the genome of *N. punctiforme* contains eight open reading frames encoding 12 domains with such photocycles (Figure 1). As in the *all1069* gene product,[44] we found an example of a bilin-binding, red-absorbing domain that was photochemically inert on a time scale of seconds (NpF2164g5). NpF2164g5 exhibits intense red fluorescence comparable to that of photochemically compromised alleles of phytochromes and CBCRs.[37,51] In the *NpF2164* gene product, this domain lies between the photochemically active NpF2164g4 and NpF2164g6 CBCRs, raising the possibility that NpF2164g5 can transfer energy to the adjacent domains to potentiate photoconversion. Although the interdomain distances for tandem CBCRs are not yet known, this hypothesis is consistent with the blue-shifted peak absorption of NpF2164g5 (Table 1). This slight blue shift allows fluorescence emission of NpF2164g5 to retain considerable overlap with the absorption bands of the adjacent domains (Figure S8F of the Supporting Information). It will be interesting to use multidomain constructs to test this hypothesis in the future.

Previous work identified a red/orange photocycle within this subfamily.[31] We describe a similar red-shifted photoproduct in NpR1597g4. We have also characterized a member of this subfamily in which the 15*Z* dark state is blue-shifted (NpF2164g7), resulting in a previously undescribed orange/green photocycle. The mechanisms resulting in this blue-shifted dark state are not yet clear, and it will be interesting to examine this protein in more detail. These anomalous photocycles did not correlate with changes in the CD associated with the two photostates (Table 1), in contrast to the differences in photoproduct CD observed for CBCRs in the insert-Cys subfamily.[36] Instead, all proteins in this study exhibited negative CD at long wavelengths and positive CD in the Soret region (Table 1), consistent with NpR6012g4 and indicative of a predominant $\alpha$-facial disposition for the chromophore D-ring in both photostates.[37,46,49]

The similarity between the $^{15Z}P_r$ states of red/green CBCRs and those of cyanobacterial phytochromes is well established.[44,46] Although this implies a similar chromophore geometry and protonation state, the mechanism underlying the green absorption of the 15*E*-PCB photoproduct is not yet clear. In the case of AnPixJ, three factors were proposed as possible explanations: twisting of the D-ring such that it is no longer in conjugation, analogous deformation of the A-ring, and deprotonation.[44] The mechanism of twisting the bilin rings out of conjugation has been repeatedly proposed to explain the spectral shifts seen in phytochromes and CBCRs.[62−64] To date, robust evidence for such twisting has been found only in the photocycles of photoactive phycobiliproteins and a subset of DXCF CBCRs.[39,40,65−67] Both cases exhibit characteristic teal-absorbing photoproducts at 490−500 nm that are generated through deconjugation of the D-ring in a PVB chromophore.[3,39,40,65−68]

For one such CBCR, NpR5113g1, the PCB photocycle has also been described.[3] In this case, the PCB photoproduct absorbs at 516 nm, blue-shifted relative to the photoproduct of red/green CBCRs (Table 1) and implying the existence of at least weak D-ring conjugation in red/green CBCRs. Moreover, incorporation of PΦB into both NpR6012g4 and NpR4776g2 results in a significant red shift of the green-absorbing photoproduct (Table 1), indicating that the C18 side chain can participate in the $^{15E}P_g$ conjugated system and contrasting with the teal-absorbing 15*E* states of DXCF CBCRs.[40] Hence, deconjugation of the D-ring is not consistent with the known properties of the $^{15E}P_g$ photoproduct of red/green CBCRs.

Alternatively, deconjugation of the A-ring in red/green CBCRs would be expected to result in a 15*E* photoproduct having properties of a PVB adduct. Green-absorbing 15*E*-PVB photostates are known in some DXCF CBCRs, and their green absorption bands superficially resemble those of the red/green CBCRs.[3,40,44−46] However, the second (Soret) transitions of the 15*E*-PVB photostates are at shorter wavelengths (335−340 nm) than those of the 15*E*-PCB photoproducts in the same proteins (350−360 nm).[3,40] The Soret transitions of both photostates in red/green CBCRs [~358 nm (Figure 2)] are in good agreement with those of the 15*E*-PCB populations of DXCF CBCRs containing both bilins, not those of the 15*E*-PVB populations.[3,40] Thus, the absorption spectra of red/green


dx.doi.org/10.1021/bi3013565 | *Biochemistry* 2012, 51, 9667−9677

CBCRs are not consistent with deconjugation of the A-ring in the $^{15E}P_g$ photostate.

A change in protonation state seems to be most consistent with the available data, both in this work and in work on AnPixJ.[57,69] Acid-denatured red/green CBCRs in the 15*E* photostate exhibit peak absorbance in the orange region of the spectrum (Figure S6 of the Supporting Information), in agreement with those of phytochromes and of other CBCRs containing PCB adducts.[3,36,38,53,57] A photoproduct with similar absorption in the orange region is also seen in the native photocycle of NpF2164g3,[36] consistent with assignment of these photostates as arising from protonated 15*E*-PCB. It is known that deprotonated dihydrobilindiones in solution can absorb at wavelengths as short as 520 nm,[70] and bilin absorption maxima are blue-shifted under neutral denaturing conditions relative to the acidic conditions employed in this work.[53] Moreover, the p$K_a$ of the bilin ring system can be below 6,[53] so a deprotonated native species at pH 7.5 is plausible. However, this working hypothesis remains far from proven. The known heterogeneity of the 15*E* photostate[59] makes the application of NMR or vibrational spectroscopy to this problem challenging, because the presence of multiple tautomers of deprotonated PCB could give rise to N−H signals from all four bilin nitrogens. Time-resolved vibrational techniques[71,72] may allow resolution of this question if the tautomeric subpopulations have sufficiently distinct kinetics.

These studies implicate functions other than color sensing for this subfamily. Four of the newly characterized proteins are notably inefficient at binding of, or covalent linkage to, the bilin chromophore. This survey was performed with recombinant expression in *E. coli*, so we cannot rule out the possibility that cyanobacterial proteins or other physiological factors such as redox potential normally drive chromophorylation more efficiently for these CBCRs. However, the apparently poor covalent assembly of NpAF142g2 suggests that this reaction, and not bilin binding, may underlie the poor chromophorylation of such proteins. Covalent attachment at C3[1] is an intrinsic reaction of the CBCR,[3,34,35,38] so domains with slower covalent attachment could be bilin-regulated sensory domains rather than bona fide photosensors. Alternately, such domains may be cryptic photosensors unless changing physiological conditions result in elevated bilin levels. For example, turnover of phycobiliproteins occurs during differentiation of vegetative *N. punctiforme* filaments into motile hormogonia, and the *NpAF142* and *NpF2854* genes harboring two of these domains are induced during differentiation into hormogonia.[73,74] Phycobiliprotein turnover upon differentiation could well result in transient increases in the level of free bilin, allowing the individual domains NpAF142g2, NpR4776g2, and NpF2854g1 to acquire chromophore and photosensory function. These domains would then presumably play a role in activating their respective kinase output domains, as reported for a red/far-red knotless phytochrome in tandem with a red/green CBCR.[31] Increased bilin levels might even confer a photosensory function on NpR3784, which has no other known photosensory domains (Figure 1). Further studies of the interplay among these putative photosensory and bilin-binding inputs will be facilitated by our description of the individual CBCR domains.

Little is currently known about the biological functions of CBCRs in *N. punctiforme*. All of the open reading frames encoding the CBCRs characterized in this study were upregulated upon differentiation of hormogonia except for the poorly expressed *NpR3784* and *NpR4776* loci.[73,74] This suggests that most red/green sensors participate in adaptation to an unfavorable light environment. Weak constitutive expression and a lack of developmental induction were also not observed for NpCcaS (NpF3797), which is nevertheless essential for regulation of phycoerythrin accumulation in complementary chromatic acclimation.[43] It is thus possible that NpR3784 and NpR4776 may be induced under conditions that have not yet been examined. Given the phototactic properties of hormogonia and the requirement for multiple CBCRs in *Synechocystis* phototaxis,[35,56,75,76] it seems likely that some or all of the induced genes will be important for modulating phototaxis in response to different colors or intensities of light. *NpR6012* and *NpF2164* are clustered with other open reading frames exhibiting homology to bacterial chemotaxis proteins such as CheA, so either or both are likely to function as phototaxis sensors in *N. punctiforme* hormogonia.

We also demonstrate that dark reversion of the 15*E* photostate can be so rapid in red/green CBCRs as to permit their use as broadband sensors of light intensity rather than as color sensors. NpF2164g7 has a linear power response to orange light (Figure S8 of the Supporting Information) and almost no loss of photoconversion under white light compared to orange light (Figure 6). It is thus well suited to function as a power meter in light environments that contain significant fluence at wavelengths of <610 nm. The signaling state of this domain could then be combined with those of color sensors in the same protein, such as NpF2164g3 (violet/orange)[36] and NpF2164g4, to allow a single protein to integrate a wide range of information about the ambient light environment. The variable photobiological and chemical functions of red/green CBCRs make them potentially useful proteins for a wide range of emerging applications in optogenetics and synthetic biology.

## ■ ASSOCIATED CONTENT

### Supporting Information

Eight figures and one table. This material is available free of charge via the Internet at http://pubs.acs.org.

## ■ AUTHOR INFORMATION

### Corresponding Author

*Department of Molecular and Cellular Biology, 31 Briggs Hall, University of California, Davis, CA 95616. Telephone: (530) 752-1865. Fax: (530) 752-3085. E-mail: jclagarias@ucdavis.edu.

### Funding

This work was supported by a grant from the Chemical Sciences, Geosciences, and Biosciences Division, Office of Basic Energy Sciences, Office of Science, U.S. Department of Energy (Grant DE-FG02-09ER16117 to J.C.L.).

### Notes

The authors declare no competing financial interest.

## ■ ACKNOWLEDGMENTS

We thank Prof. Rei Narikawa and Prof. Masahiko Ikeuchi (University of Tokyo, Tokyo, Japan) for sharing unpublished data and helpful discussions.

## ■ ABBREVIATIONS

Δabsorbance, change in absorbance (in difference spectra, which are reported as 15*Z* - 15*E*); CBCR, cyanobacteriochrome; CD, circular dichroism; DXCF, Asp-Xaa-Cys-Phe

motif defining a subfamily of dual-Cys CBCRs; GAF, domain acronym derived from vertebrate cGMP-specific phosphodiesterases, cyanobacterial adenylate cyclases, and formate hydrogen lyase transcription activator FhlA; PCB, phycocyanobilin; PVB, phycoviolobilin; PΦB, phytochromobilin; SAR, specific absorbance ratio; TES, *N*-[tris(hydroxymethyl)methyl]-2-aminoethanesulfonic acid; X, any amino acid (in the DXCF motif).

## ■ ADDITIONAL NOTES

[a]Color definitions in this study are 300−395 nm for near UV, 395−410 nm for violet, 410−480 nm for blue, 480−520 nm for teal, 520−570 nm for green, 570−580 nm for yellow, 580−615 nm for orange, 615−685 nm for red, and 685−750 nm for far red.

[b]Throughout, we describe photocycles using a convention whereby the 15*Z* photostate is listed first;[1] thus, a red/green photocycle indicates that the 15*Z* photostate is red-absorbing and the 15*E* photostate is green-absorbing. This is in keeping with biosynthesis of the 15*Z* isomer as the precursor initially bound to the phytochrome or CBCR, even in cases in which the 15*E* isomer is thermally favored.[2]

[c]We designate the new proteins in this study using the systematic nomenclature previously used for other CBCRs from *N. punctiforme*.[3] Derived from the GenBank locus tag, this nomenclature provides a unique designation for each open reading frame in *N. punctiforme*. To designate the individual CBCRs, we simplify the locus tag to Np(F/R)XXXX (e.g., locus *Npun_F2164* is simplified to NpF2164). GAF domains that contain recognizable sequence elements of the phytochrome lineage are then numbered from the N-terminus. Thus, for the *NpF2854* locus, there are four GAF domains that show homology to phytochromes, with NpF2854g1 being the most N-terminal of these domains. For cases in which there is a single phytochrome-type GAF domain, no domain number is assigned (e.g., NpR3784). GAF domains that are only distantly related to phytochromes are explicitly excluded to minimize confusion in the four cases in which a single CBCR is found as part of a larger protein also including nonphytochrome GAF domains (NpR3784, NpR2903, NpF6362, and NpR3691).

## ■ REFERENCES


(1) Rockwell, N. C., and Lagarias, J. C. (2010) A brief history of phytochromes. *ChemPhysChem 11*, 1172−1180.

(2) Tasler, R., Moises, T., and Frankenberg-Dinkel, N. (2005) Biochemical and spectroscopic characterization of the bacterial phytochrome of *Pseudomonas aeruginosa*. *FEBS J. 272*, 1927−1936.

(3) Rockwell, N. C., Martin, S. S., Gulevich, A. G., and Lagarias, J. C. (2012) Phycoviolobilin formation and spectral tuning in the DXCF cyanobacteriochrome subfamily. *Biochemistry 51*, 1449−1463.

(4) Kehoe, D. M., and Gutu, A. (2006) Responding to color: The regulation of complementary chromatic adaptation. *Annu. Rev. Plant Biol. 57*, 127−150.

(5) Christie, J. M. (2007) Phototropin blue-light receptors. *Annu. Rev. Plant Biol. 58*, 21−45.

(6) Franklin, K. A., and Quail, P. H. (2010) Phytochrome functions in *Arabidopsis* development. *J. Exp. Bot. 61*, 11−24.

(7) Möglich, A., Yang, X., Ayers, R. A., and Moffat, K. (2010) Structure and function of plant photoreceptors. *Annu. Rev. Plant Biol. 61*, 21−47.

(8) Chaves, I., Pokorny, R., Byrdin, M., Hoang, N., Ritz, T., Brettel, K., Essen, L. O., van der Horst, G. T., Batschauer, A., and Ahmad, M. (2011) The cryptochromes: Blue light photoreceptors in plants and animals. *Annu. Rev. Plant Biol. 62*, 335−364.

(9) Gomelsky, M., and Hoff, W. D. (2011) Light helps bacteria make important lifestyle decisions. *Trends Microbiol. 19*, 441−448.

(10) Moon, Y. J., Kim, S. J., Park, Y. M., and Chung, Y. H. (2010) Sensing UV/blue: Pterin as a UV-A absorbing chromophore of cryptochrome. *Plant Signaling Behav. 5*, 1127−1130.

(11) Ortiz-Guerrero, J. M., Polanco, M. C., Murillo, F. J., Padmanabhan, S., and Elias-Arnanz, M. (2011) Light-dependent gene regulation by a coenzyme B12-based photoreceptor. *Proc. Natl. Acad. Sci. U.S.A. 108*, 7565−7570.

(12) Butler, W. L., Norris, K. H., Seigelman, H. W., and Hendricks, S. B. (1959) Detection, assay, and preliminary purification of the pigment controlling photoresponsive development of plants. *Proc. Natl. Acad. Sci. U.S.A. 45*, 1703−1708.

(13) Lagarias, J. C., and Rapoport, H. (1980) Chromopeptides from phytochrome. The structure and linkage of the Pr form of the phytochrome chromophore. *J. Am. Chem. Soc. 102*, 4821−4828.

(14) Wu, S. H., and Lagarias, J. C. (2000) Defining the bilin lyase domain: Lessons from the extended phytochrome superfamily. *Biochemistry 39*, 13487−13495.

(15) Auldridge, M. E., and Forest, K. T. (2011) Bacterial phytochromes: More than meets the light. *Crit. Rev. Biochem. Mol. Biol. 46*, 67−88.

(16) Wagner, J. R., Brunzelle, J. S., Forest, K. T., and Vierstra, R. D. (2005) A light-sensing knot revealed by the structure of the chromophore binding domain of phytochrome. *Nature 438*, 325−331.

(17) Essen, L. O., Mailliet, J., and Hughes, J. (2008) The structure of a complete phytochrome sensory module in the Pr ground state. *Proc. Natl. Acad. Sci. U.S.A. 105*, 14709−14714.

(18) Yang, X., Kuk, J., and Moffat, K. (2008) Crystal structure of *Pseudomonas aeruginosa* bacteriophytochrome: Photoconversion and signal transduction. *Proc. Natl. Acad. Sci. U.S.A. 105*, 14715−14720.

(19) Kidd, D. G., and Lagarias, J. C. (1990) Phytochrome From the Green Alga *Mesotaenium caldariorum*: Purification and Preliminary Characterization. *J. Biol. Chem. 265*, 7029−7035.

(20) Yeh, K.-C., Wu, S.-H., Murphy, J. T., and Lagarias, J. C. (1997) A cyanobacterial phytochrome two-component light sensory system. *Science 277*, 1505−1508.

(21) Davis, S. J., Vener, A. V., and Vierstra, R. D. (1999) Bacteriophytochromes: Phytochrome-like photoreceptors from nonphotosynthetic eubacteria. *Science 286*, 2517−2520.

(22) Leblanc, C., Falciatore, A., Watanabe, M., and Bowler, C. (1999) Semi-quantitative RT-PCR analysis of photoregulated gene expression in marine diatoms. *Plant Mol. Biol. 40*, 1031−1044.

(23) Bhoo, S. H., Davis, S. J., Walker, J., Karniol, B., and Vierstra, R. D. (2001) Bacteriophytochromes are photochromic histidine kinases using a biliverdin chromophore. *Nature 414*, 776−779.

(24) Giraud, E., Fardoux, J., Fourier, N., Hannibal, L., Genty, B., Bouyer, P., Dreyfus, B., and Vermeglio, A. (2002) Bacteriophytochrome controls photosystem synthesis in anoxygenic bacteria. *Nature 417*, 202−205.

(25) Froehlich, A. C., Noh, B., Vierstra, R. D., Loros, J., and Dunlap, J. C. (2005) Genetic and molecular analysis of phytochromes from the filamentous fungus *Neurospora crassa*. *Eukaryotic Cell 4*, 2140−2152.

(26) De Riso, V., Raniello, R., Maumus, F., Rogato, A., Bowler, C., and Falciatore, A. (2009) Gene silencing in the marine diatom *Phaeodactylum tricornutum*. *Nucleic Acids Res. 37*, e96.

(27) Rockwell, N. C., Su, Y. S., and Lagarias, J. C. (2006) Phytochrome structure and signaling mechanisms. *Annu. Rev. Plant Biol. 57*, 837−858.

(28) Hughes, J. (2010) Phytochrome three-dimensional structures and functions. *Biochem. Soc. Trans. 38*, 710−716.

(29) Song, C., Psakis, G., Lang, C., Mailliet, J., Gartner, W., Hughes, J., and Matysik, J. (2011) Two ground state isoforms and a chromophore D-ring photoflip triggering extensive intramolecular changes in a canonical phytochrome. *Proc. Natl. Acad. Sci. U.S.A. 108*, 3842−3847.

(30) Yang, X., Ren, Z., Kuk, J., and Moffat, K. (2011) Temperature-scan cryocrystallography reveals reaction intermediates in bacteriophytochrome. *Nature 479*, 428−432.

(31) Chen, Y., Zhang, J., Luo, J., Tu, J. M., Zeng, X. L., Xie, J., Zhou, M., Zhao, J. Q., Scheer, H., and Zhao, K. H. (2012) Photophysical

diversity of two novel cyanobacteriochromes with phycocyanobilin chromophores: Photochemistry and dark reversion kinetics. *FEBS J. 279*, 40−54.
(32) Ulijasz, A. T., Cornilescu, G., von Stetten, D., Kaminski, S., Mroginski, M. A., Zhang, J., Bhaya, D., Hildebrandt, P., and Vierstra, R. D. (2008) Characterization of two thermostable cyanobacterial phytochromes reveals global movements in the chromophore-binding domain during photoconversion. *J. Biol. Chem. 283*, 21251−21266.
(33) Anders, K., von Stetten, D., Mailliet, J., Kiontke, S., Sineshchekov, V. A., Hildebrandt, P., Hughes, J., and Essen, L. O. (2011) Spectroscopic and photochemical characterization of the red-light sensitive photosensory module of Cph2 from *Synechocystis* PCC 6803. *Photochem. Photobiol. 87*, 160−173.
(34) Yoshihara, S., Shimada, T., Matsuoka, D., Zikihara, K., Kohchi, T., and Tokutomi, S. (2006) Reconstitution of blue-green reversible photoconversion of a cyanobacterial photoreceptor, PixJ1, in phycocyanobilin-producing *Escherichia coli*. *Biochemistry 45*, 3775−3784.
(35) Ikeuchi, M., and Ishizuka, T. (2008) Cyanobacteriochromes: A new superfamily of tetrapyrrole-binding photoreceptors in cyanobacteria. *Photochem. Photobiol. Sci. 7*, 1159−1167.
(36) Rockwell, N. C., Martin, S. S., Feoktistova, K., and Lagarias, J. C. (2011) Diverse two-cysteine photocycles in phytochromes and cyanobacteriochromes. *Proc. Natl. Acad. Sci. U.S.A. 108*, 11854−11859.
(37) Rockwell, N. C., Njuguna, S. L., Roberts, L., Castillo, E., Parson, V. L., Dwojak, S., Lagarias, J. C., and Spiller, S. C. (2008) A second conserved GAF domain cysteine is required for the blue/green photoreversibility of cyanobacteriochrome Tlr0924 from *Thermosynechococcus elongatus*. *Biochemistry 47*, 7304−7316.
(38) Ishizuka, T., Kamiya, A., Suzuki, H., Narikawa, R., Noguchi, T., Kohchi, T., Inomata, K., and Ikeuchi, M. (2011) The Cyanobacteriochrome, TePixJ, Isomerizes Its Own Chromophore by Converting Phycocyanobilin to Phycoviolobilin. *Biochemistry 50*, 953−961.
(39) Enomoto, G., Hirose, Y., Narikawa, R., and Ikeuchi, M. (2012) Thiol-Based Photocycle of the Blue and Teal Light-Sensing Cyanobacteriochrome Tlr1999. *Biochemistry 51*, 3050−3058.
(40) Rockwell, N. C., Martin, S. S., and Lagarias, J. C. (2012) Mechanistic Insight into the Photosensory Versatility of DXCF Cyanobacteriochromes. *Biochemistry 51*, 3576−3585.
(41) Kehoe, D. M., and Grossman, A. R. (1996) Similarity of a Chromatic Adaptation Sensor to Phytochrome and Ethylene Receptors. *Science 273*, 1409−1412.
(42) Hirose, Y., Shimada, T., Narikawa, R., Katayama, M., and Ikeuchi, M. (2008) Cyanobacteriochrome CcaS is the green light receptor that induces the expression of phycobilisome linker protein. *Proc. Natl. Acad. Sci. U.S.A. 105*, 9528−9533.
(43) Hirose, Y., Narikawa, R., Katayama, M., and Ikeuchi, M. (2010) Cyanobacteriochrome CcaS regulates phycoerythrin accumulation in *Nostoc punctiforme*, a group II chromatic adapter. *Proc. Natl. Acad. Sci. U.S.A. 107*, 8854−8859.
(44) Narikawa, R., Fukushima, Y., Ishizuka, T., Itoh, S., and Ikeuchi, M. (2008) A novel photoactive GAF domain of cyanobacteriochrome AnPixJ that shows reversible green/red photoconversion. *J. Mol. Biol. 380*, 844−855.
(45) Zhang, J., Wu, X. J., Wang, Z. B., Chen, Y., Wang, X., Zhou, M., Scheer, H., and Zhao, K. H. (2010) Fused-gene approach to photoswitchable and fluorescent biliproteins. *Angew. Chem., Int. Ed. 49*, 5456−5458.
(46) Kim, P. W., Freer, L. H., Rockwell, N. C., Martin, S. S., Lagarias, J. C., and Larsen, D. S. (2012) Femtosecond Photodynamics of the Red/Green Cyanobacteriochrome NpR6012g4 from *Nostoc punctiforme*. 1. Forward Dynamics. *Biochemistry 51*, 608−618.
(47) Altschul, S. F., Madden, T. L., Schaffer, A. A., Zhang, J., Zhang, Z., Miller, W., and Lipman, D. J. (1997) Gapped BLAST and PSI-BLAST: A new generation of protein database search programs. *Nucleic Acids Res. 25*, 3389−3402.
(48) Edgar, R. C. (2004) MUSCLE: Multiple sequence alignment with high accuracy and high throughput. *Nucleic Acids Res. 32*, 1792−1797.
(49) Rockwell, N. C., Shang, L., Martin, S. S., and Lagarias, J. C. (2009) Distinct classes of red/far-red photochemistry within the phytochrome superfamily. *Proc. Natl. Acad. Sci. U.S.A. 106*, 6123−6127.
(50) Gambetta, G. A., and Lagarias, J. C. (2001) Genetic engineering of phytochrome biosynthesis in bacteria. *Proc. Natl. Acad. Sci. U.S.A. 98*, 10566−10571.
(51) Fischer, A. J., Rockwell, N. C., Jang, A. Y., Ernst, L. A., Waggoner, A. S., Duan, Y., Lei, H., and Lagarias, J. C. (2005) Multiple roles of a conserved GAF domain tyrosine residue in cyanobacterial and plant phytochromes. *Biochemistry 44*, 15203−15215.
(52) Berkelman, T. R., and Lagarias, J. C. (1986) Visualization of bilin-linked peptides and proteins in polyacrylamide gels. *Anal. Biochem. 156*, 194−201.
(53) Shang, L., Rockwell, N. C., Martin, S. S., and Lagarias, J. C. (2010) Biliverdin amides reveal roles for propionate side chains in bilin reductase recognition and in holophytochrome assembly and photoconversion. *Biochemistry 49*, 6070−6082.
(54) Glazer, A. N., and Fang, S. (1973) Chromophore content of blue-green algal phycobiliproteins. *J. Biol. Chem. 248*, 659−662.
(55) Blot, N., Wu, X. J., Thomas, J. C., Zhang, J., Garczarek, L., Bohm, S., Tu, J. M., Zhou, M., Ploscher, M., Eichacker, L., Partensky, F., Scheer, H., and Zhao, K. H. (2009) Phycourobilin in trichromatic phycocyanin from oceanic cyanobacteria is formed post-translationally by a phycoerythrobilin lyase-isomerase. *J. Biol. Chem. 284*, 9290−9298.
(56) Yoshihara, S., Katayama, M., Geng, X., and Ikeuchi, M. (2004) Cyanobacterial Phytochrome-like PixJ1 Holoprotein Shows Novel Reversible Photoconversion Between Blue- and Green-absorbing Forms. *Plant Cell Physiol. 45*, 1729−1737.
(57) Narikawa, R., Kohchi, T., and Ikeuchi, M. (2008) Characterization of the photoactive GAF domain of the CikA homolog (SyCikA, Slr1969) of the cyanobacterium *Synechocystis* sp. PCC 6803. *Photochem. Photobiol. Sci. 7*, 1253−1259.
(58) Kim, P. W., Freer, L. H., Rockwell, N. C., Martin, S. S., Lagarias, J. C., and Larsen, D. S. (2012) Second-Chance Initiation Dynamics of the Cyanobacterial Photocycle in the NpR6012 GAF4 Domain of Nostoc Punctiforme. *J. Am. Chem. Soc. 134*, 130−133.
(59) Kim, P. W., Freer, L. H., Rockwell, N. C., Martin, S. S., Lagarias, J. C., and Larsen, D. S. (2012) Femtosecond Photodynamics of the Red/Green Cyanobacteriochrome NpR6012g4 from *Nostoc punctiforme*. 2. Reverse Dynamics. *Biochemistry 51*, 619−630.
(60) Lamparter, T., and Michael, N. (2005) *Agrobacterium* phytochrome as an enzyme for the production of ZZE bilins. *Biochemistry 44*, 8461−8469.
(61) Fischer, A. J., and Lagarias, J. C. (2004) Harnessing phytochrome's glowing potential. *Proc. Natl. Acad. Sci. U.S.A. 101*, 17334−17339.
(62) Ishizuka, T., Narikawa, R., Kohchi, T., Katayama, M., and Ikeuchi, M. (2007) Cyanobacteriochrome TePixJ of *Thermosynechococcus elongatus* harbors phycoviolobilin as a chromophore. *Plant Cell Physiol. 48*, 1385−1390.
(63) Ulijasz, A. T., Cornilescu, G., von Stetten, D., Cornilescu, C., Velazquez Escobar, F., Zhang, J., Stankey, R. J., Rivera, M., Hildebrandt, P., and Vierstra, R. D. (2009) Cyanochromes are blue/green light photoreversible photoreceptors defined by a stable double cysteine linkage to a phycoviolobilin-type chromophore. *J. Biol. Chem. 284*, 29757−29772.
(64) Ulijasz, A. T., Cornilescu, G., Cornilescu, C. C., Zhang, J., Rivera, M., Markley, J. L., and Vierstra, R. D. (2011) Structural basis for the photoconversion of a phytochrome to the activated Pfr form. *Nature 463*, 250−254.
(65) Zhao, K. H., Haessner, R., Cmiel, E., and Scheer, H. (1995) Type I Reversible Photochemistry of Phycoerythrocyanin Involves Z/E-Isomerization of Alpha-84 Phycoviolobilin Chromophore. *Biochim. Biophys. Acta 1228*, 235−243.
(66) Zhao, K. H., and Scheer, H. (1995) Type I and Type II Reversible Photochemistry of Phycoerythrocyanin α-Subunit from *Mastigocladus laminosus* both Involve Z, E Isomerization of

Phycoviolobilin Chromophore and Are Controlled by Sulfhydryls in Apoprotein. *Biochim. Biophys. Acta 1228*, 244−253.
(67) Schmidt, M., Patel, A., Zhao, Y., and Reuter, W. (2007) Structural basis for the photochemistry of α-phycoerythrocyanin. *Biochemistry 46*, 416−423.
(68) Alvey, R. M., Biswas, A., Schluchter, W. M., and Bryant, D. A. (2011) Attachment of noncognate chromophores to CpcA of *Synechocystis* sp. PCC 6803 and *Synechococcus* sp. PCC 7002 by heterologous expression in *Escherichia coli*. *Biochemistry 50*, 4890−4902.
(69) Fukushima, Y., Iwaki, M., Narikawa, R., Ikeuchi, M., Tomita, Y., and Itoh, S. (2011) Photoconversion mechanism of a green/red photosensory cyanobacteriochrome AnPixJ: Time-resolved optical spectroscopy and FTIR analysis of the AnPixJ-GAF2 domain. *Biochemistry 50*, 6328−6339.
(70) Kufer, W., Cmiel, E., Thummler, F., Rudiger, W., Schneider, S., and Scheer, H. (1982) Studies on Plant Bile-Pigments. 2. Regioselective Photochemical and Acid-Catalyzed Z,E Isomerization of Dihydrobilindione as Phytochrome Model. *Photochem. Photobiol. 36*, 603−607.
(71) Dasgupta, J., Frontiera, R. R., Taylor, K. C., Lagarias, J. C., and Mathies, R. A. (2009) Ultrafast excited-state isomerization in phytochrome revealed by femtosecond stimulated Raman spectroscopy. *Proc. Natl. Acad. Sci. U.S.A. 106*, 1784−1789.
(72) Yang, Y., Linke, M., von Haimberger, T., Hahn, J., Matute, R., Gonzalez, L., Schmieder, P., and Heyne, K. (2012) Real-time tracking of phytochrome's orientational changes during Pr photoisomerization. *J. Am. Chem. Soc. 134*, 1408−1411.
(73) Campbell, E. L., Summers, M. L., Christman, H., Martin, M. E., and Meeks, J. C. (2007) Global gene expression patterns of *Nostoc punctiforme* in steady-state dinitrogen-grown heterocyst-containing cultures and at single time points during the differentiation of akinetes and hormogonia. *J. Bacteriol. 189*, 5247−5256.
(74) Campbell, E. L., Christman, H., and Meeks, J. C. (2008) DNA microarray comparisons of plant factor- and nitrogen deprivation-induced hormogonia reveal decision-making transcriptional regulation patterns in *Nostoc punctiforme*. *J. Bacteriol. 190*, 7382−7391.
(75) Song, J. Y., Cho, H. S., Cho, J. I., Jeon, J. S., Lagarias, J. C., and Park, Y. I. (2011) Near-UV cyanobacteriochrome signaling system elicits negative phototaxis in the cyanobacterium *Synechocystis* sp. PCC 6803. *Proc. Natl. Acad. Sci. U.S.A. 108*, 10780−10785.
(76) Savakis, P., De Causmaecker, S., Angerer, V., Ruppert, U., Anders, K., Essen, L. O., and Wilde, A. (2012) Light-induced alteration of c-di-GMP level controls motility of *Synechocystis* sp. PCC 6803. *Mol. Microbiol. 85*, 239−251.